

**ANALYSIS OF PRODUCTION OF FORWARD-ANGLE FRAGMENTS  
IN THE  $^{22}\text{Ne}$  (40 AMeV) +  $^9\text{Be}$  REACTION**

**G. Kaminski<sup>1,2</sup>, A. G. Artyukh<sup>1</sup>, A. Budzanowski<sup>2</sup>, B. Erdemchimeg<sup>1,3</sup>,  
S. A. Klygin<sup>1</sup>, G. A. Kononenko<sup>1</sup>, E. Kozik<sup>2</sup>, T. I. Mikhailova<sup>1</sup>,  
Yu. M. Sereda<sup>1,4</sup>, Yu. G. Teterev<sup>1</sup>, M. Veselsky<sup>5</sup>, A. N. Vorontzov<sup>1,4</sup>**

<sup>1</sup>*Joint Institute for Nuclear Research, Dubna, Moscow Region, Russia*

<sup>2</sup>*Institute of Nuclear Physics PAN, Krakow, Poland*

<sup>3</sup>*Mongolian National University, Nuclear Research Center, Ulan-Baator, Mongolia*

<sup>4</sup>*Institute for Nuclear Research, National Academy of Sciences of Ukraine, Kyiv, Ukraine*

<sup>5</sup>*Institute of Physics, Slovak Academy of Sciences, Bratislava, Slovakia*

A mechanisms of production of forward-emitted fragments in the  $^{22}\text{Ne}$  (40 AMeV) +  $^9\text{Be}$  reaction are investigated. Inclusive velocity and isotopic distributions of products with  $3 \leq Z \leq 11$  were measured on the fragment separator COMBAS. The contribution of direct processes and dissipative ones is presented. Gaussian fitting functions according to Goldhaber formalism has been used to estimate direct components of fragments velocity distributions. Experimental data have been compared to geometric incomplete fusion model predictions. Incomplete fusion model was the first time applied for light nuclei as in the studied reaction system. Overall agreement of simulations with experiment in description of velocity distributions have been achieved for fragments with atomic number close to the projectile mass and for stable isotopes. Discrepancies for other products are the result of transition from incomplete fusion to direct processes with collisions of clusters in the participant zone.

### 1. Introduction

Intermediate energy region and especially the Fermi energy vicinity is seen as the transition region which links low and high energies phenomena. Obviously, heavy ion collisions at these energies are complex processes being a mixture of low energy dissipative binary processes and multifragmentation [1, 2]. Momentum and velocity transfer data obtained in inverse kinematics reactions demonstrate presence of projectile breakup, quasi-elastic peripheral collisions and complete/incomplete fusion at semi central collisions [3 - 6].

Projectile-like fragments (PLFs) are effectively observed in measurement performed at forward angles [3, 7, 8]. They have velocity distributions centered at velocities close to that of the projectile. Study of the inclusive velocity spectra provides important information about the undergoing processes. Spectra are characterized by Gaussian like shape with a tail at lower velocities. The problem of proper disentangling of processes corresponding to the low and high energy regimes complicates the description of experimentally measured observables in the frame of a theory. This problem was met e.g. in Refs. [9, 10] where a similar system  $^{18}\text{O}$  (35 AMeV) + Be was analyzed using Quantum Molecular Dynamics (QMD) and Boltzmann - Nordheim - Vlasov (BNV) models. It was shown that not all experimental observables can be described; peaks of simulated velocity distributions are shifted towards lower velocities. Nevertheless, both models provide a reasonably good description of dissipative component. Since

there is no universal theoretical approach which can be applied to reactions at Fermi energies to explain phenomena occurring both at low and at high energies, one can use two models to study direct and dissipative processes separately.

In this paper we present measured inclusive velocity and isotopic distributions of  $^{22}\text{Ne}$  (40 AMeV) + Be reaction products compared to independent-particle [11] and incomplete fusion (ICF) [12] models. Gaussian fits have been applied to estimate breakup products, whereas ICF model has been used for those produced in quasi-elastic transfer and inelastic collisions.

### 2. Experimental details

Experimental data were measured at the separator COMBAS of FLNR, JINR [13] used in a double achromatic spectrometry mode. A 40 AMeV  $^{22}\text{Ne}$  beam was used to bombard  $^9\text{Be}$  (14 mg/cm<sup>2</sup>) target. Fragments produced at the production target and emitted around 0°, within the angular acceptance of  $\theta \approx \pm 2.5^\circ$  and  $\varphi \approx \pm 2.0^\circ$ , were collected and transported to an achromatic focal plane ( $F_a$ ). At a dispersive focal plane ( $F_d$ ) the momentum acceptance was set to be 0.15 %.

Velocity distributions of fragments were measured by scanning over the range of magnetic rigidities  $0.5 \leq B\rho/B\rho_{\text{beam}} \leq (2.05)$ , corresponding to 1.01 - 4.14 Tm. Products were detected at the achromatic focal plane ( $F_a$ ) using  $\Delta E_1$ ,  $\Delta E_2$  (0.38 mm, 60 × 60 mm<sup>2</sup>),  $E_3$  (3.7 mm, Ø 60 mm) and E (7.5 mm, Ø 60 mm) setup of silicon detectors. Isotopic yields were obtained by summation of the

velocity spectra over the whole range of the measured velocities. The accuracy of the experimental data was limited by two factors: the statistics and the accuracy of the determination of the charge of the ion beam passing through the target. The estimated maximum error connected with beam monitoring was not greater than 15 - 20 %. Further, the yields of all the isotopes are represented in relative units after normalization of registered isotopic events to the beam monitor counts.

### 3. Reaction models

Two different theoretical approaches have been applied to give an explanation of production of forward emitted fragments in the  $^{22}\text{Ne}$  (40 A MeV) +  $^9\text{Be}$  reaction. At relativistic energies, velocity distributions of PLFs have symmetric Gaussian form. The width of Gaussian peak has been discussed with respect to the Fermi motion of nucleons in Goldhaber paper [11]. We applied Gaussian fit to the high velocity part of fragments velocity distributions to separate direct component.

A hybrid phenomenological approach of incomplete-fusion (ICF) model combined with deep-inelastic transfer (DIT) code of Tassan-Got and Stefan [14] has been used to estimate deep inelastic transfer and processes corresponding to more central collisions for description of experimental data. It was the first attempt to test the ICF model for such light reaction system like represented by  $^{22}\text{Ne} + ^9\text{Be}$ . General assumptions of the model are tailored for massive nuclei and the application of the model for reaction with  $^9\text{Be}$  nucleus as a target was under a question.  $^9\text{Be}$  is a light nucleus, moreover it has a clustered structure [15]. However, we have decided to test ICF model predictions, especially to assess dissipative processes, taking into account, that it gives a reasonably good description of the experimental data for Sn + Al and Kr + Sn systems around 20 - 25 A MeV [12, 16, 17].

In the frame of hybrid DIT + ICF model a nucleus-nucleus collision is considered as a several stages process, where each stage is treated separately. Initially a pre-equilibrium emission is considered and projectile- and target-like prefragments are reconstructed. Then two different reaction schemes can be distinguished; peripheral collisions and violent ones at small impact parameters. In each event, after the pre-equilibrium stage, DIT code is used and the overlap zone of the colliding nuclei is determined. If the overlap does not exceed 3 fm, di-nuclear quasi-projectile and quasi-target configuration is created. Otherwise an incomplete fusion channel based on the geometrical fragmentation with spectator-participant concept is realized. The main point in ICF regime is the

assumption of binary collision as a fusion of the participant zone with one of the spectators, generally the heavier one.

The deexcitation of the hot primary fragments created in DIT/ICF calculations is simulated by the statistical multifragmentation model (SMM) code [18] and its Fermi breakup subroutine [19] for products with atomic number  $A \leq 16$ .

### 4. Results and discussion

In Fig. 1 simulations of velocity distributions of fragments with  $3 \leq Z \leq 11$  using DIT + ICF/SMM are compared to the experiment. The total number of DIT + ICF/SMM events is  $5 \cdot 10^7$ . The considered events are limited to fragments emitted at the  $\theta_{\text{lab}} \leq 3^\circ$ . The angle of  $3^\circ$  is chosen to improve statistics of unstable nuclei. In the presented DIT + ICF/SMM calculations only projectile-like fragments are considered. The target-like fragments have small contribution to the total yields of studied isotopes (see e.g., [3]) being restricted by the experimental conditions (separator acceptance, the range of measured velocities) and will be omitted in analysis. All calculated yields are normalized to  $^{20}\text{F}$  yield.

The measured velocity distributions of all fragments have asymmetric form with the maximum peaked close to the beam velocity position. The fast velocity component can be attributed to direct breakup and quasi-elastic transfer reactions. Both mechanisms are present in this transition collision energy domain. DIT + ICF/SMM gives a fairly good description for products with masses close to that of the projectile. In this mass region peripheral collisions give the main contribution and model used here reproduces DIT processes. Thus, the calculated spectra have maxima shifted towards lower values. On the contrary, experimental distributions of fragments with mass  $A < 22$  are peaked in the range of 0.94 - 1.02 of beam velocity ( $V_{\text{beam}}$ ) whereas DIT + ICF/SMM gives about 1 % of velocity loss per a removed nucleon starting from maximum value of  $0.97 V_{\text{beam}}$ . This shift demonstrates that fast fragments are produced in fragmentation processes. Breakup component was separated by fitting the right side of velocity distribution by function  $Ce^{-(v-v_0)/2\sigma^2}$ , where  $C$  – is normalization parameter,  $v_0$  is the most probable peak value in the distribution,  $\sigma_{\square}(v_{\text{rel}})$  is half width of velocity distribution. Examples of these fits are shown in Fig. 2, *a*.

The distribution of widths  $\sigma_{\square}(v_{\text{rel}})$  of fragments compared to the formulation by Goldhaber converted to width of  $v_{\text{rel}} = v_{\text{prod}}/v_{\text{beam}}$  units are shown in Fig. 2, *b*. The Goldhaber curve is as follows,

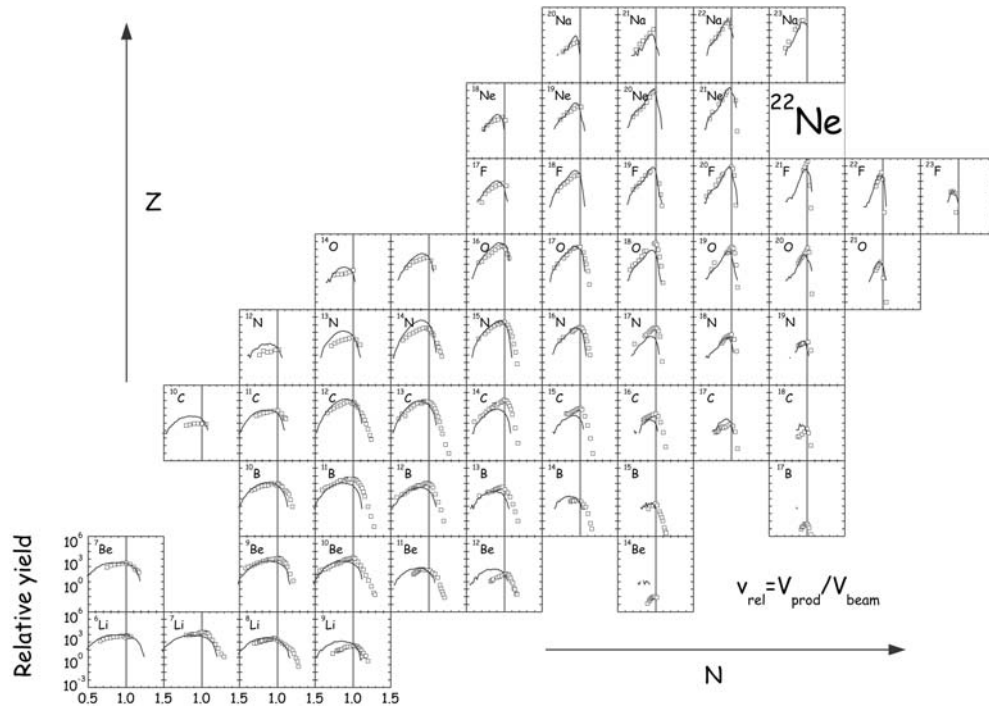


Fig. 1. Forward-angle inclusive velocity distributions of the reaction products. Relative velocity is the ratio of the velocity of product to the beam velocity. Symbols are experimental data, lines are calculations. Vertical lines indicate the beam velocity.

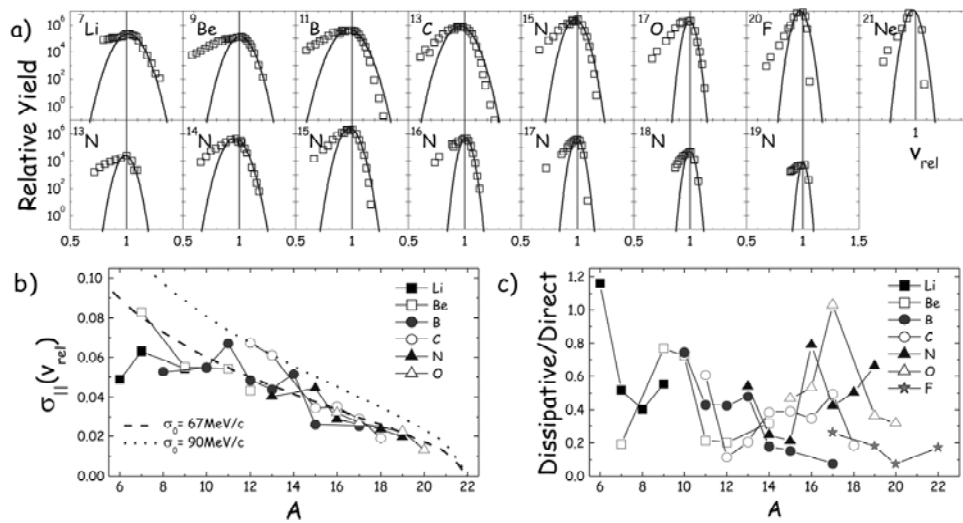


Fig. 2. Gaussian fit of high velocity part of the distributions of stable and nitrogen isotopes. Squares represent experimental data, dashed line - Gaussian fit (a). Relative velocity width of direct component. The dashed and short dashed curves are for reduced width  $\sigma_0 = 67$  MeV/c and 90 MeV/c, respectively (b). Ratio of the estimated yield of dissipative to direct processes of selected isotopes (c).

$$\sigma_{\parallel}(v_{rel}) = \sigma_0 \cdot \sqrt{\frac{A_f(A_p - A_f)}{(A_p - 1)}} / (A_f \cdot m_p \cdot \beta_{beam}),$$

where  $A_{p,f}$  is the mass number of the projectile and fragment, respectively,  $m_p$  is the proton mass in MeV/c<sup>2</sup>,  $\beta_{beam} = v_{beam}/c$ . We obtained the reduced width  $\sigma_0 = 67$  MeV/c from the experimental results instead of 90 MeV/c from the experiments at relativistic energies.

Experimental value of  $\sigma_0$  is about 20 MeV/c

lower than predicted by theory [11], which is in accordance with other groups [20]. This can be explained, taking into account the simplicity of Goldhaber formalism, in which correlations between nucleons and Pauli correlations are not included. Only kinematics correlations are taken into account.

An asymmetry and a long tail in the low velocities side result from dissipative processes of low-energy reactions. Moving from the projectile mass to light elements mass region the contribution

of inelastic part systematically increases, the distributions are wider and more asymmetrical. In Fig. 2, *c* ratio of experimental dissipative to Gaussian component is presented. Most fragments are characterized by the ratio smaller than 0.6. All elements except fluorine isotope chains have local maxima around stable isotopes. An interesting feature is the same influence on the total yield of  $^{17}\text{O}$  isotope of both components.

Fig. 3 show the calculated dissipative components of stable and nitrogen isotopes compared to the experimental ones. DIT +

+ ICF/SMM calculations reproduce satisfactory dissipative part of the spectra of stable products, as incomplete fusion scenario is applied.

In Fig. 4 both DIT/ICF+SMM and experimental isotopic distributions are presented. Experimental spectra are characterized by the bell-like shapes with maximum yield which corresponds to isotopes with mass around the stability line isotopes. DIT/ICF+SMM simulations give the overestimated yields of proton-rich isotopes, comparable to the experimental yields for stable isotopes and underestimation of neutron-rich fragments.

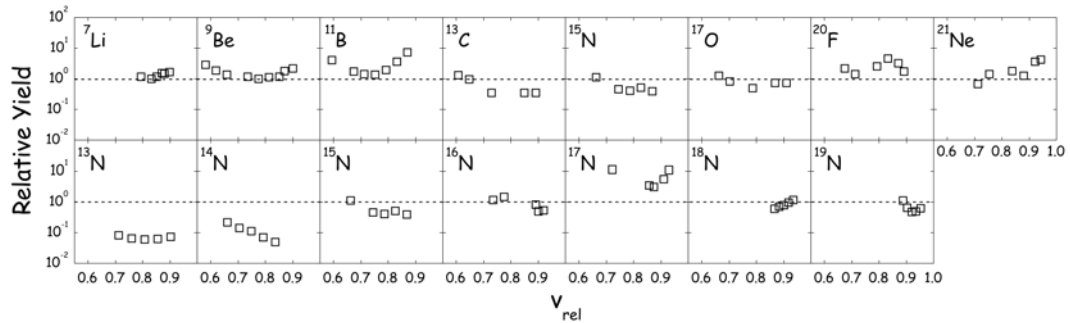


Fig. 3. Ratio of the estimated experimental dissipative parts of velocity spectra to the calculated one ( $Y_{\text{exp}}/Y_{\text{cal}}$ ) for stable and nitrogen isotopes, respectively.

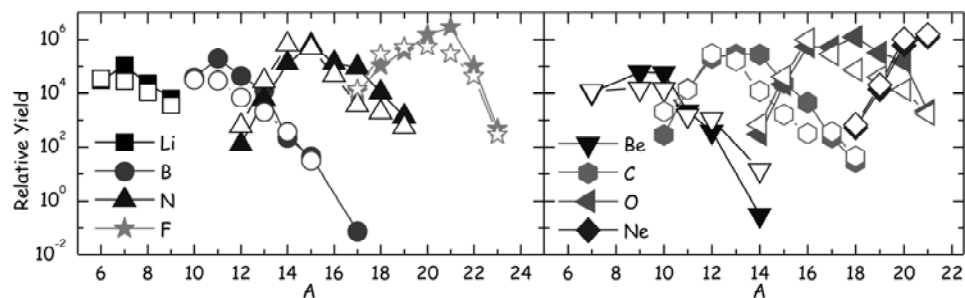


Fig. 4. Isotopic distribution, full symbols are experimental data, empty are DIT/ICF + SMM calculations.

According to the model assumptions, the clusters in participant zone fuse with projectile which becomes heavier and hotter. This gives the final products that are less neutron-rich because of de-excitation stage. Unlike the neutron-rich isotopes, proton-rich fragments are overestimated. In experiment, it is much more probable that the participant clusters will go away by themselves and the products remain cold and neutron-rich. The discrepancies are substantial for  $^{18}\text{O}$ ,  $^{17}\text{N}$ ,  $^{14}\text{C}$ ,  $^{15}\text{C}$ , which are analogous to projectile minus  $1\alpha$ ,  $1\alpha + 1p$ ,  $2\alpha$ ,  $2\alpha + n$ . Due to cluster structure, instead of fusing with projectile, the clusters in participant zone collide with the clusters in the projectile and the rest of the projectile just follows the initial trajectory. Observed discrepancies between theory and experiment can be attributed to the transition from the incomplete-fusion to direct processes with collisions of clusters in the participant zone.

## 5. Conclusions

Two different theoretical approaches have been applied to describe experimental data for the  $^{22}\text{Ne}$  (40 AMeV) +  $^9\text{Be}$  reaction. According to Goldhaber formalism the contribution of direct processes to the production mechanism of forward emitted fragments has been evaluated. We have obtained the reduced width  $\sigma_0 = 67$  MeV/c. The lower than expected ( $\sim 90$  MeV/c) value of  $\sigma_0$  can be explained by the simplicity of the theory, where correlations between nucleons are not taken into account. Most fragments (quasi-elastic transfer, breakup). Nevertheless, considerable contributions from dissipative processes are found for isotopes around the stability line. The hybrid model gives a reasonably good description of quasi-elastic transfer reactions (DIT code) for products with mass close to that of the projectile and incomplete fusion of component for

stable elements. For other fragments ICF does not reproduce the experimental results. It is understandable, when assuming that the main assumption of the model of incomplete fusion is not fulfilled. Nevertheless, the difference of experimental data versus model calculations can provide

the systematics of the excess of direct neutron-rich (cold) component, which emerges instead of slow proton-rich (hot).

This work has been partially supported by the Slovak Scientific Grant Agency under Grant No. A-1266. VEGA-2/0073/08.

## REFERENCES

1. *Gregoire C., Tamain B.* Intermediate energy heavy ion reactions // *Ann. Phys. Fr.* - 1986. - Vol. 11. - P. 323 - 455.
2. *Fuchs H., Moring K.* Heavy-ion break-up processes in the Fermi energy range // *Rep. Prog. Phys.* - 1994. - Vol. 57. - P. 231 - 324.
3. *Dayras R., Pagano A., Barrette J. et al.* Peripheral interactions for  $^{44}\text{MeV/u } ^{49}\text{Ar}$  on  $^{27}\text{Al}$  and  $^{\text{nat}}\text{Ti}$  Targets // *Nucl. Phys.* - 1986. - Vol. A460. - P. 299 - 323.
4. *Faure-Ramstein B., Auger F., Wieleczko J.P. et al.* // *Nucl. Phys.* - 1995. - Vol. A586. - P. 533 - 556.
5. *Hanold K.A., Bazin D., Mohar M.F. et al.* Heavy residues from very mass-asymmetric heavy-ion reactions // *Phys. Rev.* - 1995. - Vol. C52. - P. 1462 - 1483.
6. *Notani M., Sakurai H., Aoi N. et al.* Projectile fragmentation reactions and production of nuclei near the neutron drip line // *Phys. Rev.* - 2007. - Vol. C76. - P. 044605-1 - 044605-15.
7. *Souliotis G.A., Morrissey D.J., Orr N.A. et al.*  $0^\circ$  measurements of momentum distributions of projectile-like fragments // *Phys. Rev.* - 1992. - Vol. C46. - P. 1383 - 1392.
8. *Pfaff R., Morrissey D.J., Fauerbach M. et al.* Projectilelike fragment momentum distributions from  $^{86}\text{Kr} + \text{Al}$  at 70 MeV/nucleon // *Phys. Rev.* - 1995. - Vol. C51. - P. 1348 - 1355.
9. *Artukh A.G., Budzanowski A., Kamiński G. et al.* QMD approach in description of the  $^{18}\text{O} + ^9\text{Be}$  and  $^{18}\text{O} + ^{181}\text{Ta}$  reactions at  $E_{\text{proj}} = 35$  A MeV // *Acta Phys. Pol.* - 2006. - Vol. B37. - P. 1875 - 1892.
10. *Mikhailova T., Colonna M., Di Toro M. et al.* Investigations of dissipative collisions with transport models // *Rom. Journ. Phys.* - 2007. - Vol. 32. - P. 875 - 893.
11. *Goldhaber A.S.* Statistical model of fragmentation processes // *Phys. Lett.* - 1974 - Vol. B53. - P. 306 - 308.
12. *Veselsky M.* Production mechanism of hot nuclei in violent collisions in the Fermi energy domain // *Nucl. Phys.* - 2002. - Vol. A705. - P. 193 - 222.
13. *Artukh A.G., Gridniev G.F., Grushezhki M. et al.* Wide aperture separator COMBAS realized on the strong focusing principle // *Nucl. Instr. Meth.* - 1999. - Vol. A426. - P. 605 - 617.
14. *Tassan-Got L., Stefan C.* // *Nucl. Phys.* - 1991. - Vol. A524. - P. 121 - 140.
15. *Von Oertzen W., Freer M., Kanada-En'yo Y.* Nuclear clusters and nuclear molecules // *Phys. Rep.* - 2006. - Vol. 432. - P. 43 - 113.
16. *Veselsky M., Souliotis G.A., Chubarian G. et al.* Heavy residues with  $A < 90$  from the asymmetric reaction of 20 A MeV  $^{124}\text{Sn} + ^{27}\text{Al}$  as a sensitive probe of the onset of multifragmentation // *Nucl. Phys.* - 2003. - Vol. A724. - P. 431 - 454.
17. *Veselsky M., Souliotis G.A.* Production of cold fragments in nucleus-nucleus collisions in the Fermi-energy domain // *Nucl. Phys.* - 2007. - Vol. A781. - P. 521 - 530.
18. *Bondorf J.P., Botvina A.S., Iljinov A.S. et al.* Statistical multifragmentation of nuclei // *Phys. Rep.* - 1995. - Vol. 257. - P. 133 - 221.
19. *Botvina A.S., Iljinov A.S., Mishustin I.N. et al.* Statistical simulation of the break-up of highly excited nuclei // *Nucl. Phys.* - 1987. - Vol. A475. - P. 663 - 686.
20. *Lahmer W., von Oertzen W., Miczaika A. et al.* Transfer and fragmentation reactions of  $^{14}\text{N}$  at 60 MeV/u // *Z. Phys. A* - 1990. - Vol. 337. - P. 425 - 437.

### АНАЛІЗ ВИХОДІВ ФРАГМЕНТІВ, ЩО ВИПРОМІНЮЮТЬСЯ ПІД НУЛЬОВИМИ КУТАМИ, В РЕАКЦІЇ $^{22}\text{Ne}$ (40 MeV/A) + $^9\text{Be}$

Г. Камінські, А. Г. Артюх, А. Будзановські, Б. Ердечимег, С. А. Ключін,  
Г. А. Кононенко, Е. Козік, Т. І. Міхайлова,  
Ю. М. Серета, Ю. Г. Тетерев, М. Весельські, А. Н. Воронцов

Досліджується механізм утворення фрагментів, що випромінюються під нульовими кутами в реакції  $^{22}\text{Ne}$  (40 MeV/A) +  $^9\text{Be}$ . За допомогою сепаратора фрагментів COMBAS виміряно інклюзивні швидкісні, ізотопні і зарядові розподіли фрагментів реакції з  $3 \leq Z \leq 11$ . Для опису периферійних реакцій було використано модель глибоко непружних передач, а для опису більш центральних зіткнень модель неповного злиття. При описі розподілів за швидкостями фрагментів з атомними номерами, близькими до налітаючого іона, отримано хороше узгодження розрахованих та експериментальних даних, тоді як для більш віддалених фрагментів спостерігається розходження результатів розрахунків та експерименту. Спостерігається еволюція механізму утворення, що дає вклад у повний вихід випромінюваних ізотопів із збільшенням числа нуклонів, що відриваються від ядра налітаючого іона.

**АНАЛИЗ ВЫХОДОВ ФРАГМЕНТОВ, ИСПУЩЕННЫХ ПОД НУЛЕВЫМИ УГЛАМИ,  
В РЕАКЦИИ  $^{22}\text{Ne}$  (40 МэВ/А) +  $^9\text{Be}$**

**Г. Камински, А. Г. Артюх, А. Будзановски, Б. Эрдемчимег, С. А. Ключин,  
Г. А. Кононенко, Э. Козик, Т. И. Михайлова,  
Ю. М. Серда, Ю. Г. Тетерев, М. Весельски, А. Н. Воронцов**

Исследуется механизм образования фрагментов в реакции  $^{22}\text{Ne}$  (40 МэВ/А) + Be, испущенных под нулевыми углами. С помощью сепаратора фрагментов COMBAS измерены инклюзивные скоростные, изотопные и зарядовые распределения фрагментов реакции с  $3 \leq Z \leq 11$ . Для описания периферических реакций использовалась модель глубоко-неупругих передач, а для описания более центральных столкновений – модель неполного слияния. При описании распределений по скоростям фрагментов с атомными номерами, близкими к налетающему иону, получено хорошее согласие расчетных и экспериментальных данных, тогда как для более удаленных фрагментов наблюдается расхождение расчетов и эксперимента. Наблюдается эволюция механизма образования, дающая вклад в полный выход изучаемых изотопов с увеличением числа нуклонов, отрываемых от ядра налетающего иона.

Received 09.06.08,  
revised - 22.12.08.